

Volume electric dipole origin of second-harmonic generation from metallic membrane with non-centrosymmetry patterns

Yong Zeng and Jerome V. Moloney

Arizona Center for Mathematical Sciences, University of Arizona, Tucson, Arizona 85721

In this article, we analytically study second harmonic (SH) generation from thin metallic films with subwavelength, non-centrosymmetry patterns. Because the thickness of the film is much smaller than the SH wavelength, retardation effects are negligible. The far-field SH intensities are thus dominated by an effective electric dipole. These analytical observations are further justified numerically by studying the effect of polarization of the fundamental field on both the SH signal and the electric dipole. It is demonstrated that bulk SH polarization density is comparable with its surface counterpart. The electric dipole, consequently, originates from the entire *volume* of the metallic membrane, in contrast to the fact that SH generation from metal surface is generally dominated by a *surface* dipole. © 2018 Optical Society of America

OCIS codes: 160.4330, 190.3970, 260.5740

Optical second-harmonic generation (SHG) from one-dimensional metal surfaces were first observed in 1965 [1], and attracted considerable attentions in the following fifty years (see Ref. [2, 3] and the cited references). Recently, scientific interests have gradually shifted to the quadratic nonlinearities of membrane-like metal films with subwavelength, non-centrosymmetry patterns, partially owing to the significant near-field enhancement induced by the excitation of localized plasmon resonances [4–6]. On the experimental side, SHG was observed from different geometric configurations such as split-ring resonators [7, 8] and their complementary counterparts [9], noncentrosymmetric T-shaped nanodimers [10], T-shaped [8] and L-shaped nanoparticles [11, 12].

For ideally infinite metal surfaces, it is well known that the dominant second-harmonic (SH) electric dipole source appears only at the interface between centrosymmetric media where the inversion symmetry is broken. Higher order multipole sources, such as magnetic dipole and electric quadrupole, merely provide a relatively small bulk SH polarization density. In contrast to an infinite surface, we will show in this article that there are *volume* electric dipoles which dominate SHG from thin metal films with non-centrosymmetry patterns. The underlying physical reasons include: (1) the non-centrosymmetry patterns allow SH electric dipoles to appear in the overall structure [13, 14]; and (2) the thickness of the film is far smaller than the SH wavelength thus retardation effects are negligible.

In general, SH radiation of a patterned structure satisfies the following inhomogeneous wave equation [15],

$$\nabla \times \nabla \times \mathbf{E}(\omega) - \frac{\omega^2}{c^2} \mathbf{E} = i\omega\mu_0 f(\mathbf{r}) \mathbf{j}(\mathbf{r}, \omega), \quad (1)$$

where $f(\mathbf{r})$ stresses the structural geometry: it equals 1 for metal and 0 for vacuum. We now consider an ideal current sheet whose thickness (along z direction) $d_z \ll \lambda$ with λ being the SH wavelength. The SH electric field at direction \mathbf{n} in the far zone is found to be [16]

$$\mathbf{E} = \frac{ik\eta}{4\pi r} e^{ikr} (\mathbf{n} \times \mathbf{p}) \times \mathbf{n}, \quad (2)$$

with $\eta = \sqrt{\mu_0/\epsilon_0}$ and

$$\mathbf{p}(\mathbf{n}) = \int \int \mathbf{j}(\mathbf{r}_{\parallel}, z) e^{-ik(\mathbf{n}_{\parallel} \cdot \mathbf{r}_{\parallel} + n_z z)} d\mathbf{r}_{\parallel} dz. \quad (3)$$

Here $k = 2\pi/\lambda$ is the wave number in vacuum, and the integration is performed over the volume of the sheet. At either positive or negative z direction, we have

$$\mathbf{E} = \frac{ik\eta}{4\pi r} e^{ikr} \mathbf{p}_{\parallel}(\mathbf{n}). \quad (4)$$

The far-zone field is therefore transverse with a vanishing z component. Without loss of generality, we choose the electric field along the x direction (namely, $\mathbf{p}_{\parallel} = p_{\parallel} \mathbf{e}_x$). The associated

SH intensity is thus proportional to

$$\begin{cases} \left| \int_0^{d_z} g(z) e^{-ikz} dz \right|^2 & \text{at } +z \text{ direction;} \\ \left| \int_0^{d_z} g(z) e^{ikz} dz \right|^2 & \text{at } -z \text{ direction,} \end{cases} \quad (5)$$

where the integral function

$$g(z) = \int j_x(\mathbf{r}_{\parallel}, z) d\mathbf{r}_{\parallel} \quad (6)$$

stands for the total current at a specific z plane.

To identify the contributions of different order multipole sources, we expand Eq.(5) in a power series of kd_z [15]. At the leading order, the intensities at the $\pm z$ directions are identical and proportional to

$$\left| \int_0^{d_z} g(z) dz \right|^2 = \left| \int \int j_x(\mathbf{r}_{\parallel}, z) d\mathbf{r}_{\parallel} dz \right|^2. \quad (7)$$

The right-hand side of Eq.(7) is the total current of the sheet or equivalently the effective *electric dipole*. At the first order of kd_z , these two signals have a difference of

$$2ik \int_0^{d_z} \int_0^{d_z} g(z_1) g^*(z_2) (z_1 - z_2) dz_1 dz_2, \quad (8)$$

and the associated relative difference reads as

$$\text{Im} \left\{ \frac{-4k \int_0^{d_z} g(z) z dz}{\int_0^{d_z} g(z) dz} \right\}. \quad (9)$$

In other words, the difference is induced by the appearance of magnetic dipole and electric quadrupole. Their influence is negligible under the conditions such as (1) complex $g(z)$ with slowly-varying phase, or (2) $d_z/\lambda \ll 1$, or (3) $g(z)$ is symmetrical such that $g(z) = g(d_z - z)$; or (4) $g(z)$ is localized at one point (such as SHG from metal surface). On the other hand, $g(z)$ with rapid-varying phase, such as a nonlocal electric dipole, can lead to a remarkable difference [13, 17, 18]. However, we will show it is unlikely to happen in an ideally thin film.

To numerically study second-order nonlinearities of thin metallic films, we employ a classical model developed recently [3, 9]. This model has been demonstrated to not only provide qualitative agreement with experiments, but also reproduce the overall strength of the experimentally observed SH signals. Before we present the numerical results, it should be stressed that, as suggested by simulations (not shown here), these results are quite general and can be found from different configurations including (1) perfect T-shaped, C-shaped and L-shaped patterns; (2) ideal C_{1v} -symmetric patterns supported by semi-infinite dielectric substrate; (3) asymmetric pattern with perturbed C_{1v} -symmetry; and (4) particle arrays with size-tolerance disorder.

The representative film studied here is a freestanding array of gold split-ring resonators with a thickness of 25 nm, which closely matches the experimental sample in Ref. [7–9]. Schematic drawing of this patterned film is shown in Figure 1, together with its linear spectra. In the following, we choose a fundamental-frequency (FF) field which propagates along the z direction and has a wavelength of 1212 nm. This wavelength corresponds to the valley in the transmission which is induced by the fundamental plasmonic resonance [19].

Figure 2 shows the effect of the incident polarization angle θ on both the far-zone SH electric field as well as the total SH current. The distinct dependence between the different component of the SH electric field can be interpreted in terms of the electric dipole approximation [3]. The most striking feature is that almost identical SH electric fields, with a relative difference as small as 0.5%, are found along the $(\pm z)$ directions. Moreover, the amplitude of the electric dipole is proportional to the SH electric fields. Consequently, SH radiation from this thin film is dominated by the electric dipole defined in Eq.(7), and higher-order multipoles can be safely neglected. It should be mentioned that the same observations are also experimentally found from an individual metal tip: the emission of SH radiation at the tip can be attributed to a single on-axis oscillating dipole [20,21].

To explore the characteristics of the electric dipole, the spatial distribution of j_y with a x -polarized illumination is calculated ($\theta = 0$ therefore $j_x = 0$) and plotted in Figure 3, at a time corresponding to a maximal j_y . We further define the following functions

$$\begin{aligned} g(z) &= \sum_{x,y} j_y(x, y, z), & g_s(z) &= \sum_{z' \leq z} g(z'); \\ l(x) &= \sum_y j_y(x, y, z_0), & l_s(x) &= \sum_{x' \leq x} l(x'); \end{aligned} \quad (10)$$

with $z_0 = 12.5$ nm. Here $g(z')$ stands for the total current at the $z = z'$ plane, and $l(x')$ represents the sum of j_y along the line $(x = x', z = z_0)$. $g_s(z)$ is a cumulative function with $g_s(z_{max})$ corresponding to the electric dipole. Clearly, the $g(z)$ here is almost symmetrical in z , mainly because the film thickness is so thin that both FF and SH fields are nearly constant inside the film. In other words, the retardation effects are negligible. As discussed previously, it is this symmetrical $g(z)$ which results in the negligible higher-order multipoles. On the other hand, each element of the metal volume contributes to the SH radiation, in a constructive/destructive way. Assuming the outermost grid layer (a finite-difference time-domain method is utilized here [3]) constitutes the metal surface (its 2.5-nm thickness is much thicker than a *real* surface), then the internal bulk polarization density is found to be comparable with its surface counterpart. As a consequence, the effective electric dipole originates from the entire metal *volume*. In addition, SH current distribution on the $z = 12.5$ nm plane is shown in Fig. (3c). Around the inner corners, the current is found to be strongly depolarized and form localized bright hot spots. This phenomenon has been observed from

metal surfaces with nanoscale roughness, and the origin is attributed to the overlap between SH and fundamental modes [22, 23].

We now discuss the experiment reported in Ref. [11] where considerable multipole interferences, in addition to the dominant electric dipole, were observed. The experimental sample is a 20-nm-thick gold film periodically perforated with an L-shaped pattern, and the FF wavelength is 1060 nm. The phase variation of the FF wave inside the metal is small, approximately 0.01π , which should result in a $g(z)$ quite close to the one shown in Fig. (3a). Consequently, the multipole contribution should be negligible. The difference between experiment and theory is believed to be induced by sample imperfections which may result in strongly localized out-of-phase currents at *both* (according to the condition (4) mentioned above) top and bottom metal-dielectric interfaces. On the other hand, we want to point out that significant multipole sources may appear in large-size metal particles [13, 17] and multilayered structures such as bulk photonic metamaterials [24].

The authors thank Stephan W. Koch and Colm Dineen for their helpful comments. This work is supported by the Air Force Office of Scientific Research (AFOSR), under Grant No. FA9550-07-1-0010 and FA9550-04-1-0213. J. V. Moloney acknowledges support from the Alexander von Humboldt foundation.

References

1. F. Brown, R. E. Parks and A. M. Sleeper, Phys. Rev. Lett. 14, 1029 (1965).
2. A. Liebsch, *Electronic Excitations at Metal Surfaces* (Plenum press, 1997).
3. Y. Zeng, W. Hoyer, J. Liu, S. W. Koch, and J. V. Moloney, Submitted, also at arXiv:0807.3575.
4. K. Busch, G. von Freymann, S. Linden, S. F. Mingalaevev, L. Tkeshelashvili, and M. Wegener, Phys. Rep. 444, 101 (2007).
5. A. Nahata, R. A. Linke, T. Ishi, and K. Ohashi, Opt. Lett. 28, 423 (2003).
6. M. D. McMahon, R. Lopez, R. F. Haglund, E. A. Ray, and P. H. Bunton, Phys. Rev. B 73, 041401(R) (2006).
7. M. W. Klein, C. Enkrich, M. Wegener, and S. Linden, Science 313, 502 (2006).
8. M. W. Klein, M. Wegener, N. Feth, and S. Linden, Opt. Express 15, 5238 (2007).
9. N. Feth, S. Linden, M. W. Klein, M. Decker, F. Niesler, Y. Zeng, W. Hoyer, J. Liu, S. W. Koch, J. V. Moloney, and M. Wegener, Opt. Lett. 33, 1975 (2008).
10. B. K. Canfield, H. Husu, J. Laukkanen, B. Bai, M. Kuittinen, J. Turunen, and M. Kauranen, Nano Lett. 7, 1251 (2007).
11. S. Kujala, B. K. Canfield, M. Kauranen, Y. Svirko, and J. Turunen, Phys. Rev. Lett. 98, 167403 (2007).
12. S. Kujala, B. K. Canfield, M. Kauranen, Y. Svirko, and J. Turunen, Opt. Express, 16, 17196 (2008).
13. J. I. Dadap, J. Shan, and T. F. Heinz, J. Opt. Soc. Am. B 21, 1328 (2004).
14. M. Finazzi, P. Biagiona, M. Celebrano, and L. Duò, Phys. Rev. B 76, 125414 (2007).
15. J. D. Jackson, *Classical Electrodynamics* (Second edition, John Wiley & Sons, 1975).
16. Y. Zeng and J. V. Moloney, Opt. Lett. In Press (2009), also at arXiv:0903.0663.
17. J. I. Dadap, J. Shan, K. B. Eisenthal, and T. F. Heinz, Phys. Rev. Lett. 83, 4045 (1999).
18. G. Bachelier, I. Russier-Antoine, E. Benichou, C. Jonin, and P. F. Brevet, J. Opt. Soc. Am. B 25, 955 (2008).
19. C. Rockstuhl, F. Lederer, C. Etrich, Th. Zentgraf, J. Kuhl, and H. Giessen, Opt. Express 14, 8827 (2006).
20. A. Bouhelier, M. Beversluis, A. Hartschuh, and L. Novotny, Phys. Rev. Lett. 90, 013903 (2003).
21. J. Nappa, G. Revillod, I. Russier-Antoine, E. Benichou, C. Jonin, and P. F. Brevet, Phys. Rev. B 71, 165407 (2005).
22. C. Anceau, S. Brasselet, J. Zyss, and P. Gadenne, Opt. Lett. 28, 713 (2003).
23. M. I. Stockman, D. J. Bergman, C. Anceau, S. Brasselet, and J. Zyss, Phys. Rev. Lett. 92, 057402 (2004).

24. E. Kim, F. Wang, W. Wu, Z. Yu, and Y. R. Shen, Phys. Rev. B 78, 113102 (2008).

References

1. F. Brown, R. E. Parks, A. M. Sleeper, “Nonlinear Optical Reflection from a Metallic Boundary”, *Phys. Rev. Lett.* 14, 1029 (1965).
2. A. Liebsch, *Electronic Excitations at Metal Surfaces* (Plenum press, 1997).
3. Y. Zeng, W. Hoyer, J. Liu, S. W. Koch, J. V. Moloney, “A classical theory for second-harmonic generation from metallic nanoparticles”, Submitted, also at arXiv:0807.3575.
4. K. Busch, G. von Freymann, S. Linden, S. F. Mingalaeiev, L. Tkeshelashvili, and M. Wegener, “Periodic nanostructures for photonics”, *Phys. Rep.* 444, 101 (2007).
5. A. Nahata, R. A. Linke, T. Ishi, K. Ohashi, “Enhanced nonlinear optical conversion from a periodically nanostructured metal film”, *Opt. Lett.* 28, 423 (2003).
6. M. D. McMahon, R. Lopez, R. F. Haglund, E. A. Ray, P. H. Bunton, “Second-harmonic generation from arrays of symmetric gold nanoparticles”, *Phys. Rev. B* 73, 041401(R) (2006).
7. M. W. Klein, C. Enkrich, M. Wegener, S. Linden, “Second-Harmonic Generation from Magnetic Metamaterials,” *Science* 313, 502 (2006).
8. M. W. Klein, M. Wegener, N. Feth, S. Linden, “Experiments on second- and third-harmonic generation from magnetic metamaterials”, *Opt. Express* 15, 5238 (2007).
9. N. Feth, S. Linden, M. W. Klein, M. Decker, F. Niesler, Y. Zeng, W. Hoyer, J. Liu, S. W. Koch, J. V. Moloney, and M. Wegener, “Second-harmonic generation from complementary split-ring resonators”, *Opt. Lett.* 33, 1975 (2008).
10. B. K. Canfield, H. Husu, J. Laukkanen, B. Bai, M. Kuittinen, J. Turunen, M. Kauranen, “Local field asymmetry drives second-harmonic generation in noncentrosymmetric nanodimers,” *Nano Lett.* 7, 1251 (2007).
11. S. Kujala, B. K. Canfield, M. Kauranen, Y. Svirko, J. Turunen, “Multipole Interference in the Second-Harmonic Optical Radiation from Gold Nanoparticles”, *Phys. Rev. Lett.* 98, 167403 (2007).
12. S. Kujala, B. K. Canfield, M. Kauranen, Y. Svirko, J. Turunen, “Multipolar analysis of second-harmonic radiation from gold nanoparticles”, *Opt. Express*, 16, 17196 (2008).
13. J. I. Dadap, J. Shan, T. F. Heinz, “Theory of optical second-harmonic generation from a sphere of centrosymmetric material: small-particle limit”, *J. Opt. Soc. Am. B* 21, 1328 (2004).
14. M. Finazzi, P. Biagiona, M. Celebrano, L. Duò, “Selection rules for second-harmonic generation in nanoparticles”, *Phys. Rev. B* 76, 125414 (2007).
15. J. D. Jackson, *Classical Electrodynamics* (Second edition, John Wiley & Sons, 1975).
16. Y. Zeng and J. V. Moloney, ”Polarization-Current-Based, finite-difference time-domain, Near-to-Far-Field Transformation”, *Opt. Lett.* In Press (2009), also at arXiv:0903.0663.

17. J. I. Dadap, J. Shan, K. B. Eisenthal, T. F. Heinz, “Second-Harmonic Rayleigh Scattering from a Sphere of Centrosymmetric Material”, *Phys. Rev. Lett.* 83, 4045 (1999).
18. G. Bachelier, I. Russier-Antoine, E. Benichou, C. Jonin, P. F. Brevet, “Multipolar second-harmonic generation in noble metal nanoparticles”, *J. Opt. Soc. Am. B* 25, 955 (2008).
19. C. Rockstuhl, F. Lederer, C. Etrich, Th. Zentgraf, J. Kuhl, and H. Giessen, “On the reinterpretation of resonances in split-ring-resonators at normal incidence”, *Opt. Express* 14, 8827 (2006).
20. A. Bouhelier, M. Beversluis, A. Hartschuh, and L. Novotny, “Near-Field Second-Harmonic Generation Induced by Local Field Enhancement”, *Phys. Rev. Lett.* 90, 013903 (2003).
21. J. Nappa, G. Revillod, I. Russier-Antoine, E. Benichou, C. Jonin, P. F. Brevet, “Electric dipole origin of the second harmonic generation of small metallic particles”, *Phys. Rev. B* 71, 165407 (2005).
22. C. Anceau, S. Brasselet, J. Zyss, P. Gadenne, “Local second-harmonic generation enhancement on gold nanostructures probed by two-photon microscopy”, *Opt. Lett.* 28, 713 (2003).
23. M. I. Stockman, D. J. Bergman, C. Anceau, S. Brasselet, J. Zyss, “Enhanced Second-Harmonic Generation by Metal Surfaces with Nanoscale Roughness: Nanoscale Dephasing, Depolarization, and Correlations”, *Phys. Rev. Lett.* 92, 057402 (2004).
24. E. Kim, F. Wang, W. Wu, Z. Yu, Y. R. Shen, “Nonlinear optical spectroscopy of photonic metamaterials”, *Phys. Rev. B* 78, 113102 (2008).

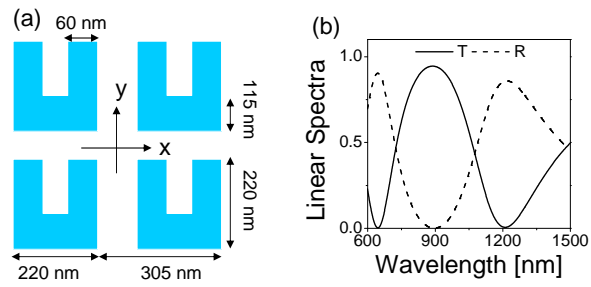


Fig. 1. (a) Schematic drawing of a square lattice of gold split-ring resonators. The thickness of the gold film is 25 nm. (b) Its linear spectra under a x -polarized normal incidence.

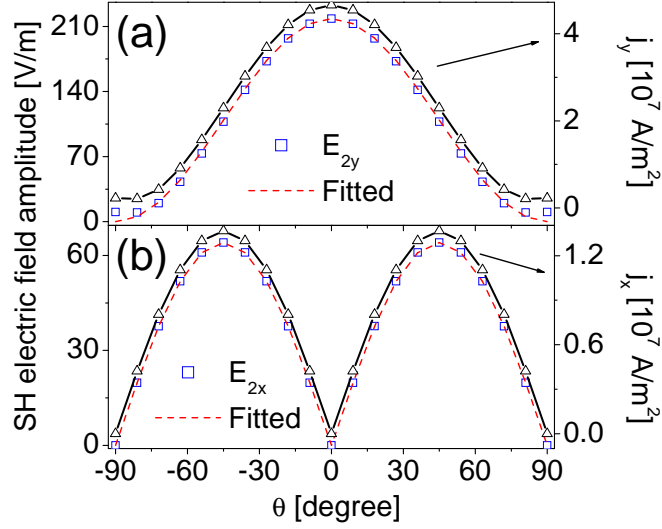


Fig. 2. The effect of incident polarization angle θ on the far-zone second harmonic electric field along the $\pm z$ direction, with $\theta = 0$ corresponding to polarization along the x direction. The fitted function employed is (a) $\cos^2 \theta$ and (b) $|\sin 2\theta|$, respectively. The averaged current density (proportional to the electric dipole) \mathbf{j} is also shown. The amplitude of the incident fundamental frequency electric field E_0 is 2×10^7 (V/m), same as that used in the experiments [7]. The bulk plasma frequency of gold is taken as $\omega_p = 1.367 \times 10^{16} \text{s}^{-1}$, the phenomenological collision frequency $\gamma = 6.478 \times 10^{13} \text{s}^{-1}$ [3].

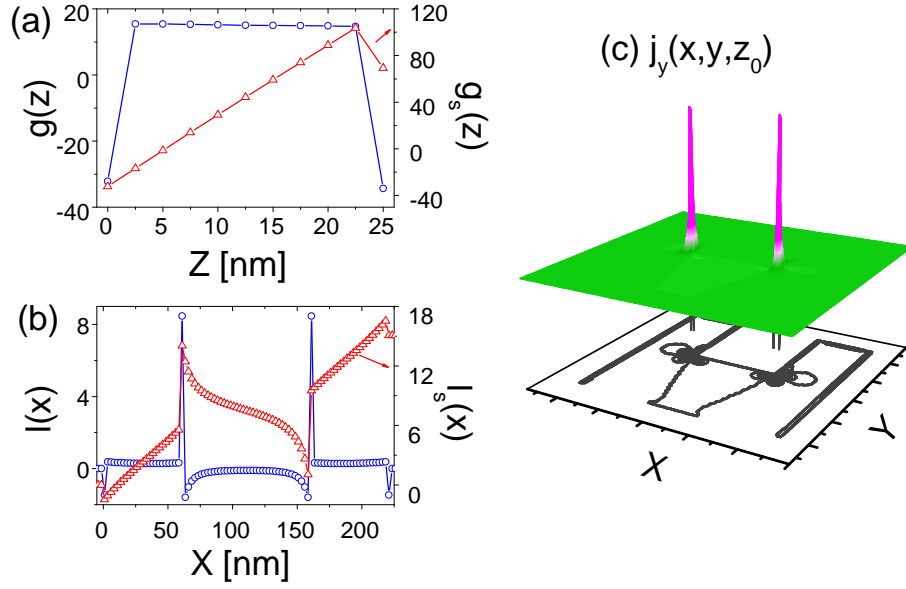


Fig. 3. The spatial distribution of second-harmonic current (with arbitrary units) with a x -polarized normal incidence. The resolution is limited to 2.5 nm due to computational resource limitations. $z(x) = 0$ corresponds to the starting plane of the gold film along the $z(x)$ direction. (c) The current distribution on the plane of $z_0 = 12.5$ nm.